



Journal of Anatomical Sciences

Email: anatomicaljournal@gmail.com

J Anat Sci 4 (2)

The Effects of STZ-Induced IDDM on Neural Crest Cell Migration and Neuroepithelial Cell Proliferation: An Immunohistochemical and Stereological Analyses Study.

Chinnah, Tudor I.

University of Exeter Medical School, St Luke's Campus, Heavitree Road, Exeter, EX1 2LU, UK. Tel: 01392 722994. Fax: 01392722926. E-mail: T.I.Chinnah@exeter.ac.uk.

ABSTRACT

Diabetes-induced congenital malformations commonly affect organs and tissues that are derived from ectomesenchymal cells, such as the neural tube and cardiovascular structures. Human diabetic pregnancy has also been strongly associated with DiGeorge anomaly, Goldenhar and the axial mesodermal dysplasia syndromes. The cellular and molecular mechanisms of these malformations are still poorly understood, including their effects on the migration and proliferation of the ectomesenchymal-derived cells. Diabetes (IDDM) was induced in female MF1 mice with 150mg/kg of Streptozotocin one week before mating. Pregnancy was terminated on E9.5, E10, E11 or E12 and the embryos were examined for gross structural malformations. The distributions of immunoreactivity for migrating neural crest cells, permissive ECM substrate molecules (fibronectin and laminin) and proliferating cells were investigated in histological sections of the malformed embryos. The absolute number of migrated cells in the trigeminal ganglion was also stereologically estimated. It could not be deduced from the results that the diabetic milieu directly affected the migratory pattern of the cranial neural crest cells and ECM molecules along the migratory pathways. However, the proliferative cycle and interkinetic migration of neuroepithelial cells were distorted in the malformed embryos from the diabetic mice. An average deficit of 11.2%-13.5% in the estimated absolute number of cells in the trigeminal ganglion was also observed. It is probable that the teratogenic effects of the diabetic state involve inhibition of the developmental processes of ectomesenchymal cells, including progenitor cells' differentiation and cell proliferation, through interference with the expression of a variety of the cells' developmental regulating genes and molecules.

Key words: Neural crest; Neuroepithelial; Cell migration; Proliferation; Congenital malformations.

INTRODUCTION

Maternal diabetes has long been associated with an increased risk of congenital anomalies. In humans, between 24% - 74% of insulin dependent diabetes mellitus (IDDM)-induced malformations are severe multi-organ system birth defects.^{1,2,3} Diabetes-induced congenital malformations are especially common in organs and tissues that are derived from ectomesenchymal cells, such as the neural tube and cardiovascular structures.^{4,5,6} A strong association between overt maternal diabetes and conotruncal congenital heart diseases (CHDs) such as double-outlet right ventricle and truncus arteriosus, has been demonstrated.^{7,8} A earlier study on a mouse model of diabetic pregnancy reported a high susceptibility to diabetes-induced angioblastic cell or vascular anomalies in the offspring.⁹ Ablation of the neural crest in chick embryos alters the migration of mesenchymal cells, causing anomalies of the branchial arches and ventricular out-flow tracts, in association with thymic and parathyroid agenesis.¹⁰ This malformation complex

corresponds to the DiGeorge Anomaly (DGA) in humans, which is similarly characterized by CHDs.^{11,12}

The occurrences of coincident DGA and renal agenesis in the offspring of diabetic (IDDM) mothers have been widely reported in humans.¹³ The sequence of malformations in axial mesodermal dysplasia syndrome has also been strongly associated with maternal diabetes. Congenital malformations in offspring of pregnant women with IDDM are said to show specific structural defects. These defects share phenotypic overlap with recognised patterns of malformations seen in Goldenhar syndrome and axial mesodermal dysplasia spectrum.^{6,14} It is thought that DGA, its associated cardiovascular anomalies, and the axial mesodermal dysplasia syndromes may have a common developmental pathogenesis which involves a generalised alteration in both mesodermal and cranial neural crest cells' migration.^{15,16}

Despite these interesting reports on diabetes-induced embryopathies in both human and animal models, the

cellular and molecular mechanisms of these malformations remain largely unclear. Little is known about the effects of the diabetic condition on the migration and proliferation of ectomesenchymal-derived cells, or about the role these developmental processes could play in the cascade of the mechanisms associated with diabetes-induced congenital malformations. This study therefore examined the effects of the diabetic state on the immunoreactive migrating neural crest cells, the permissive extracellular matrix (ECM) substrate molecules (fibronectin and laminin), and cell proliferation in the malformed embryos. The absolute number of cells in a neural crest cell target organ of the malformed embryos was also stereologically estimated.

MATERIALS AND METHODS

A total of 40 virgin female MF1 mice weighing between 20 - 30 gm were used. The mice were housed in controlled environmental conditions with 14-h light and 10-h dark cycles and were fed with pellet chow diet and water ad libitum. Diabetes was induced before mating by a subcutaneous injection of 150 mg/kg body weight of streptozotocin (STZ) dissolved in a sterile 0.1 M sodium citrate buffer pH 4.5 at a concentration of 10 mg/ml. Control animals were injected with equivalent volume of 0.1 M sodium citrate buffer. Diabetic animals were mated with non-diabetic males of the same strain within one day after confirmation of induced diabetes; in parallel, non-diabetic control females were also mated with non-diabetic males of the same strain. Details of how animals with induced diabetes were determined have been previously described.¹⁴ The induced serum glucose levels in the pregnant diabetic mice varied between 15 mmol/l - 27 mmol/l. Pregnancy was terminated on gestation days E9.5, E10, E11 or E12 by cervical dislocation and the embryos were harvested. Each embryo was staged for age,¹⁷ inspected for external malformations and weighed. Malformed and normal embryos from the diabetic and control groups were randomly selected for further morphological analysis.



Figure 1.
A: BBC microcomputer interfaced with a digitizing tablet and an Olympus microscope with an attached drawing tube.



B: Quantimet 970 image analyser connected to a microscope with attached camera and computer monitors.

IMMUNOHISTOCHEMISTRY

Serial sections of paraformaldehyde fixed embryos, cut with a rotary microtome at a thickness of 5 μ m, were processed for immunohistochemical staining for migrating neural crest cells, fibronectin and laminin immunoreactivity. The sections were incubated overnight at 40°C in either monoclonal anti-HNK-1/N-CAM (mouse IgM, clone V1.1) at a dilution of 1:50, or rabbit anti-human fibronectin at a dilution of 1:200, or rabbit anti-mouse laminin at a dilution of 1:500 primary antibodies (SIGMA Chemical Company). At least 6 embryos of each embryonic age (E9.5 - E12.5) were randomly chosen from 5 litters of diabetic (malformed) and non-diabetic (control) mothers. Three non-malformed embryos from the diabetic group were also randomly chosen for each embryonic age under study. The monoclonal anti-human HNK-1/N-CAM antibody visualises cell surface determinant (Human Natural Killer-1 antigen) which is a glycoprotein, (sulphate-3-glycoronyl residue) on pre-migratory and migrating neural crest cells and neural cell adhesion molecule (N-CAM). Similarly cut serial sections of methacarn fixed embryos were also processed for immunohistochemical staining for Proliferating Cells Nuclear Antigen (PCNA). The sections were also incubated overnight at 40°C in monoclonal anti-PCNA (mouse IgG, clone PC10) primary antibody (SIGMA Chemical Company) at a dilution of 1:200. This antibody recognises cell cycle-related regulatory protein involved in DNA replication.

For ease of comparison of the tissue sections, alternate slides of serial sections of blocks of the embryos stained for histopathological examination were selected for the immunohistochemical study. Also, embryonic tissue sections between the levels of easily identifiable anatomical landmarks (re the optic vesicles and the heart) were selected for consistency and comparison of identical structural regions. Sections of the embryos from diabetic mothers, malformed (DMM) and non-malformed (DMN); and normal embryos from the control group were stained together. For each antibody staining, 24 serial slide sections made of 10 slides of DMM, 4 slides of DMN, 8 slides of normal control and 2 slides of internal negative control were taken together

in one staining rack as a batch and stained at the same time for uniformity of staining reaction between groups. For each embryonic age, 5 batches of slide sections were stained.

STEREOLOGICAL ANALYSIS

Embryos of E10.5 and E11.5 were selected and processed for JB4 resin embedding for stereological estimation of absolute number of cells in the trigeminal ganglion. The fractionator method for unbiased particle counting,¹⁸ was used. Malformed (DMM) and non-malformed (DMN) embryos from diabetic mothers and normal embryos from control mothers were randomly selected from litters of at least 4 pregnant mice for each embryonic age. The resin blocks were cut with a Ralph glass knife on an LKB Historange rotary microtome at a pre-determined thickness of 2 μ m. The required microtome section thickness was determined by measurement of the diameter of the nuclear profiles of the trigeminal ganglion cells using a drawing tube attached to an Olympus (BH-2) microscope and a Calcomp 2000 digitizer tablet linked to a BBC microcomputer (fig.1A), using previously written software.¹⁹ Serial sections of the block of each embryo were cut through the whole of the trigeminal ganglion. The sections were flattened and stretched out on a water bath at room temperature. Consecutive pairs of the sections were then collected on a glass slide starting with the first section and dried on a hot plate. The sections were stained with Acid Fuchsin for 2 minutes, washed in running tap water, counterstained for 2 minutes in 0.05% Toluidine Blue and washed in running tap water. The tissue sections were air-dried and mounted with DPX.

Based on the results of a pilot study, a dissector interval of 1/50 was used as the optimal pre-determined sampling fraction for this study.²⁰ In all the sections, only the right trigeminal ganglions were counted for uniformity of assessment. Cell counting was made on pairs of sections with a Quantimet 970 image analyser (Cambridge Instrument Limited, UK) using nuclear profiles as counting units. A digital image of the trigeminal ganglion in one of the tissue sections (reference section) on the slide with a total magnification of X1650 was captured on a computer screen. An A4 acetate sheet serving as a counting sampling frame was pasted on the screen covering the entire field of view. Profiles of nuclei of the ganglion cells were traced on the acetate with a marker pen. The field of view was systematically changed such that the entire section of the trigeminal ganglion was meticulously covered with minimal overlap.

A similar procedure was carried out for cells' nuclear profiles in the second section (look-up section). The acetate sheet with the profiles from the reference section was superimposed on the acetate sheet from the look-up section with corresponding field of view. Cells' nuclear profiles that appeared on the reference sheet but not on the look-up sheet were counted and the total of

such profiles in all the sheets from the tissue section was counted as Q- for the reference section. To greatly improve the efficiency of the method, the cell counting procedure was repeated on the same pair of sections in reverse directions to obtain the count of Q- for the look-up section.²¹ The total number 'N' of the nuclear profiles in the reference or look-up sections was obtained by using the formula, $N = Q \cdot x \cdot f$, where f is the reciprocal of the sampling fraction.^{22,18} The mean of 'N' from the reference and look-up sections was recorded as the estimated absolute number of cells of the ganglion for each embryo sample.²¹

DATA ANALYSIS

Data are presented as means \pm SEM (standard error of mean). Tests of significance of difference in the medians of the parameters between groups were analysed using the Mann-Whitney U test. Correlation between variables was examined using Spearman's Rank Sum correlation test. In each case, the null hypothesis was rejected if the probability of no difference was less than 5% (i.e. $p < 0.05$). Analysis of variance (ANOVA) and Student's t-test were performed as appropriate. Differences between groups were detected by Student's t-test based on Tukey's multiple comparison test. All statistical analyses were carried out with the Minitab statistical package.

RESULTS

Neural crest cells migration

In order to understand the cellular mechanisms of diabetes-induced malformations involving ectomesenchymal-derived organs and tissues, the effects of the diabetic state on neural crest cell migration was investigated. The results showed no detectable differences in the distribution of HNK-1 positive cells between normal embryos from control and malformed embryos from diabetic mice (figures not shown). The immunoreactivity of permissive ECM substrate molecules fibronectin and laminin showed normal distribution in sections of the embryos. There was no difference between normal embryos from control and malformed embryos from diabetic mice (figures not shown).

A quantitative investigation using stereological estimation of absolute number of neurons in the trigeminal ganglion was also undertaken to explore the migration of cranial crest cells into target organs. The trigeminal ganglion is one of the cranial sensory ganglia that are target organs for migrating cranial neural crest cells. The ganglion is a well-established experimental model because it is comparatively large, has well-defined boundaries and is easily identifiable. In E10.5 mouse embryos, the ganglion extends rostrally from just above the level of the optic vesicle and caudally to the level of the otic vesicle; in E11 – 11.5 embryos, it extends from the level of optic vesicle to halfway above the level of the otic vesicle.¹⁷

As shown in table 1, there were statistically significant ($p < 0.05$) differences in the estimated absolute total

number of the trigeminal ganglion cells between age-matched normal embryos of control and malformed embryos of diabetic mice (DMM) in the ages studied. The estimated absolute total number of trigeminal ganglion cells decreased significantly in DMM embryos compared to the age-matched normal embryos of the control mice. In E10.5 DMM embryos, the number of trigeminal ganglion cells was an average of 11.2% less than in age-matched controls. In E11.5 DMM embryos it was an average of 13.5% less. The

estimated absolute total number of cells in the ganglion increased significantly ($p < 0.05$) with increase in embryonic age. The number of the ganglion cells in DMN of E10.5 embryos was higher than the DMM of the same age but was not statistically significant. In both embryonic ages, the number of ganglion cells in control and age-matched DMN embryos did not differ significantly ($p > 0.05$).

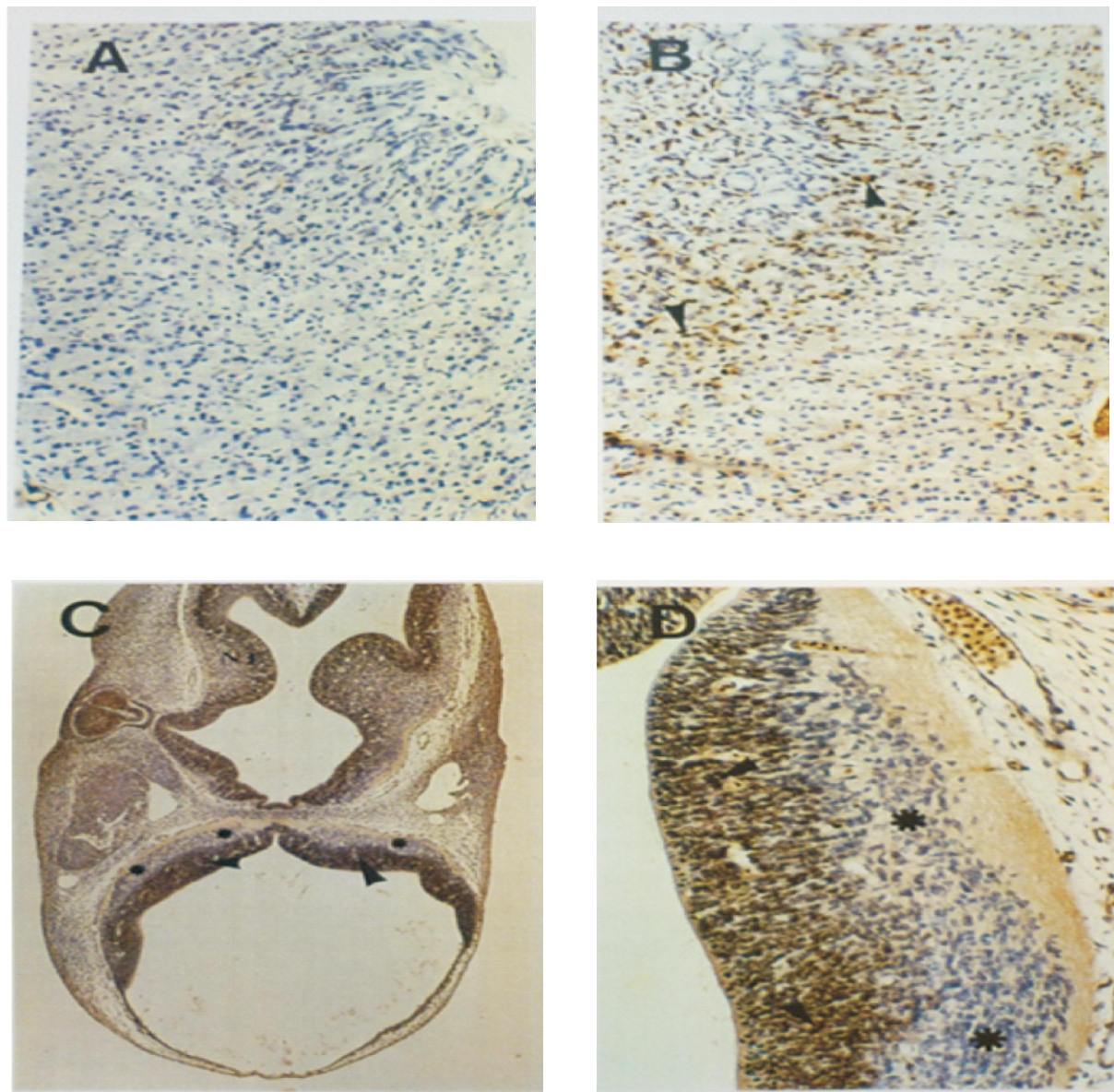


Figure 2.

A & B: Sections of adult female MF1 mouse stomach stained with PCNA to serve as negative (A) and positive (B) controls. Figure A, stained without the primary antibody, shows no non-specific immunoreactivity. Figure B shows positive (dark brown) PCNA immunoreactivity in the proliferating cells of the gastric glands (arrowheads). X 200. C: Section of an E10/10.5 normal embryo from a non-diabetic control mouse showing the general pattern of PCNA immunoreactivity. Tissues outside the neural tube show a mosaic pattern with a mixture of positively (dark brown) and negatively (pale blue) stained cells. The Neural tube (NT) shows a layer of dark brown stained inner cells (arrowheads) and a pale blue stained outer layer of cells (asterix). X 40. D: Higher magnification of a section of the neural tube of an E10/10.5 normal mouse embryo from a non-diabetic mother, showing a distinct dark brown positive PCNA stained inner layer of neuroepithelial cells (arrowheads) and negative pale blue stained outer layer of cells (asterix). X 200.

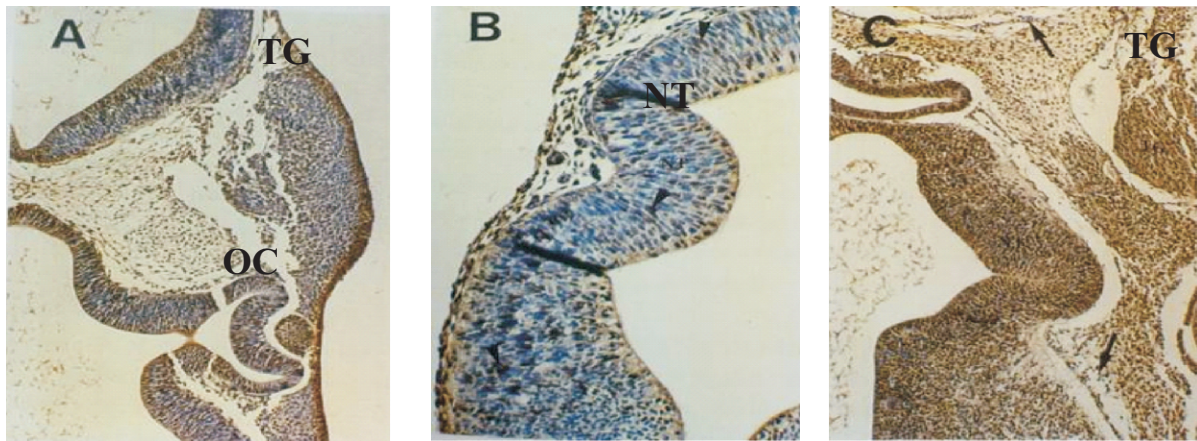


Figure 3.

A: Section of an E10/10.5 malformed mouse embryo from a diabetic mother, showing a general mosaic pattern of a mixture of positive (dark brown) and negative (pale blue) PCNA immunoreactivity, including the neural tube (NT). Cells of the trigeminal ganglion (TG) and optic cup (OC) also show mosaic positive and negative PCNA staining. X 100.

B: Higher magnification of a section of E10/10.5 malformed mouse embryo from a diabetic mother, showing a mosaic staining pattern within each layer of cells of the neural tube (NT). PCNA positive immunoreactive cells (arrowheads) show dark brown. X 200.

C: Section of an E11.5 malformed mouse embryo from a diabetic mother showing a similar mosaic pattern of PCNA immunoreactivity as in figure 3A. Angioblastic cells among the mesenchymal cells stained negative for PCNA. X 100.

Table 1: Estimated Absolute Number of the Trigeminal Ganglion Cells, Mean SEM.

	Control	DMN	DMM
E10.5	68975 ± 3710 ^a CV = 6.8% N = 5	66156 ± 4881 ^{ab} CV = 9.7% N = 4	62019 ± 2131 ^b CV = 4.7% N = 4
E11.5	89875 ± 4800 ^c CV = 6.8% N = 6	92950 ± 5138 ^c CV = 7.4% N = 4	79160 ± 5422 ^d CV = 9.6% N = 5

Data with the same letter code are not statistically significant ($p > 0.05$). CV = coefficient of variation, N = number of embryos examined. DMN = Non-malformed embryos from diabetic mice. DMM = Malformed embryos from diabetic mice.

CELL PROLIFERATION

Sections of adult female MF1 mouse stomach used as positive controls showed PCNA immunoreactivity in proliferating cells of the gastric glands (fig.2B). The negative control sections showed no immunoreactivity (fig.2A). This suggests that the primary antibody is binding specifically to the proliferating cell antigen and the secondary antibody is also binding specifically to the primary antibody as expected. PCNA immunoreactivity showed cells with strong nuclear and weak cytoplasmic staining intensity in sections of embryos from the control mice. The nuclear staining showed a mixture of diffused and granular stains in the sections (fig.2C&D). There was no difference in the staining intensity between immunoreactive cells in sections of the different embryonic ages in the control.

There was uniform layered positive and negative staining of proliferating (mitotic) cells and non-proliferating (post-mitotic) cells in the neural tube of the sections of the control embryos. The PCNA-

positive neuroepithelial cells were found in the luminal half or two-third of the tube, while PCNA-negative cells occupied the outer one-third (fig.2C&D). This reflected the stages of the neuroepithelial cells maturation in the developing neural tube. Most of the surrounding mesenchymal cells and cells of other structures in the sections of the embryos stained positive, with sparsely scattered negative cells reflecting cells at different proliferative stages as would be expected in normal developing tissues.

In the sections of malformed embryos from diabetic mice, the immunoreactivity of PCNA in the neuroepithelial cells of the neural tube showed a mosaic pattern of negatively and positively stained cells, without the defined uniform layer of staining seen in the control sections (fig. 3A, B &C). The mosaic staining pattern was also observed in most other structures to a greater extent than that observed in sections of control embryos. These include the trigeminal ganglion, optic and otic vesicles and gut tube. There were more

negatively stained cells within the surrounding mesenchymal cells and in other structures of embryos from diabetic mice than in the controls. The majority of these negatively stained cells were vascular elements or angioblastic cells. The distribution of positive PCNA immunoreactivity in DMN embryos did not differ from that found in the normal controls. The staining intensity in embryos from diabetic mice (DMM and DMN) did not differ from that found in controls. There was no noticeable difference in the number of positive PCNA immunoreactive cells in the region between the neural tube and the surface ectoderm between embryos from diabetic and non-diabetic control mice, except for the negatively stained angioblastic cells in DMM embryos.

DISCUSSION

The aim of this study was to investigate the effects of diabetic pregnancy on the migration and proliferation of ectomesenchymal-derived cells. It explored the distributions of immunoreactive migrating neural crest cells and the permissive ECM substrate molecules, fibronectin and laminin. The immunohistochemical results did not show any effect of the diabetic condition on the migration of neural crest cells. This could be because the HNK-1/N-CAM monoclonal antibody has a poor sensitivity to mouse specimens. Species differences in the sensitivity of neural crest cells and their derivatives to HNK-1 have been reported.^{23,24} Furthermore, it could not be deduced from this study whether the diabetic state induced alterations in the distributions of the permissive ECM substrate molecules along the migratory pathways of the neural crest cells.

However, the observed differences in the estimated total number of cells in the trigeminal ganglion suggests either that neural crest cells were delayed in homing-in on their target organs or that there was a reduced cell proliferation. The trigeminal ganglion cells are derived from both neural crest and placodal cell populations.^{25,26} The ganglion becomes discernible in mouse embryos by E9 and the boundaries become clearly demarcated in the embryos by E10.5 and above. Over 50% of the trigeminal ganglion neurons are lost in a phase of programmed cell death that extends from E13 to E19.²⁷ This implies that between E12 and E13 the trigeminal ganglion would have attained its maximum number of neurons. The embryonic ages when the numbers of trigeminal ganglion neurons were estimated in this study were therefore before the phase of the programmed cell death. It could be argued that the DMM embryos were growth retarded compared to the control embryos,⁹ a mechanism which could account for the reduced number of neurons in the trigeminal ganglion. However, it is well documented that in cases of growth retardation the brain growth in terms of cell number is spared.²⁸ Neuronal sparing in cases of growth retardation has also been observed in the peripheral nervous system.^{29,30} It is reasonable to suggest that the observed average deficit of 11.2% (E10.5) and 13.5%

(E11.5) in the ganglion cells of DMM embryos compared to the age matched controls could be an indication of impaired neural crest and placodal cells development occasioned by the diabetic state. This may be the result of delayed migration of these cells, inhibited cell proliferation or induced premature apoptosis.

This study also demonstrated a distinct effect of the diabetic state on cell proliferation in the neural tube. The staining pattern of sections of embryos from control and non-malformed embryos from diabetic mice showed a layered positive and negative staining of the neuroepithelial cells consistent with the proliferative cycle in neural tube histogenesis. This process produces a sheet of neuroepithelial cells displaying a gradient in cell maturation and a spatially defined proliferation compartment within the neural tube. The early neural epithelium of the neural tube consists of a homogenous population of pluripotent elongated pseudo-stratified neuroepithelial cells. These cells undergo a sequence of interkinetic migration with different phases of proliferative cycle within the developing neural tube.³¹ Throughout most of the neuraxis, proliferative cell cycles are limited to the ventricular and sub-ventricular zones.³² In this study, the region of the neural tube, which showed positive PCNA immunoreactivity in the control embryos corresponded to the ventricular and sub-ventricular zones of the developing neural tube, consistent with the expected sequence of normal neuroepithelial cell proliferative cycles within the tube.

However, in the malformed embryos of the diabetic mice, PCNA immunoreactive positive cells extended to the mantle and cortical zones, which should not have proliferating cells.^{31,32} This could imply a distortion in the normal neuroepithelial cell proliferative cycles and interkinetic migration which may predispose the embryos to neural tube defects. Disturbed cell proliferation and interkinetic migration of neuroepithelial cells was clearly demonstrated in malformed embryos of diabetic mice together with an average deficit of 11.2% - 13.5% in the estimated absolute total number of trigeminal ganglion cells. This may suggest that the diabetic state distorted or impaired neuroepithelial cell proliferation and migration. It may have also impaired the proliferation of the progenitor cells, and consequently affected differentiation and generation of neural crest cells. A possible reduction in the production of crest cells could explain in part the deficit in the number of crest cells homing-in on target organs in addition to inhibited cell proliferation. These findings are consistent with the reports of earlier studies that showed impairment in the development of neural crest cell derived cranial nerve ganglia (re V, VII - X), in rodent diabetic pregnancy.^{33,34} Distortion of neuroepithelial cells of the cranial neural tube has also been reported in embryos of diabetic mice.³⁵

Part of the developmental processes of neural

progenitor cells includes recognition and decisions about positional identity, mitotic state and the need to follow a programmed cell death path.³⁶ Impairment in the regulation of these processes could lead to neural tube defects.³⁷ Diabetic condition has been shown to affect the proliferation and apoptosis of neural progenitor cells in the developing spinal cord.³³ Such effects on the progenitor cell population could alter cell cycle kinetics and lead to maldevelopment.³⁸ Hyperglycaemia has also been found to impair the proliferation and cell fate specification of neural stem cells and has been suggested as a basis for neural tube anomalies in embryos of diabetic pregnancy.³⁹

Diabetes-induced teratogenesis has also been associated with apoptosis of other embryonic cells.^{33,40,3} This could explain why diabetic pregnancy is also strongly linked with a sequence of malformations seen in axial mesodermal dysplasia or caudal regression syndromes. In the study reported here, a general mosaic pattern of PCNA immunoreactivity was observed within and outside the neural tube of DMM embryos. This may suggest that the negatively immunoreactive embryonic cells were at non-dividing phase or that the post mitotic cells were undergoing increased cell death. The results of this study provide further evidence in support of an earlier work where diabetes was reported to have induced neuroepithelial cell cytotoxicity and angioblastic cell hyperplasia in the mouse embryos.⁹ There is growing evidence of the association of diabetic pregnancy with induced congenital malformations, suggestive of direct effects of the diabetic milieu on embryonic developmental processes.

A plethora of studies have been undertaken to understand the cellular and molecular mechanisms of the diabetes-induced malformations, and have implicated a number of genes and molecules regulating cells developmental processes. For example, increased incidence of congenital vascular defects in diabetic pregnancy has been linked with elevated diacylglycerol (DAG) levels.⁴¹ DAG is one of the cell signalling factors that works through activation of the protein kinase C (PKC) family of proteins to affect endothelial cell proliferation, cellular morphology, apoptosis and barrier function.^{42,43} RasGRP3 (Rasguanyl-releasing protein3), a Ras activator expressed in developing blood vessels, has been implicated in the mediation of diabetes-induced vascular defects. RasGRP3 requires DAG for its activity and elevated DAG in diabetic condition over activates RasGRP3, resulting in induced vascular defects.⁴⁴

Mesangial cell migration is said to be impaired in diabetic condition due to the loss of synthesis of laminin 421.⁴⁵ A selective reduction in mRNA translation of laminin B2 in the hyperglycaemic milieu has also been reported.⁴⁵ In an analysis of global gene expression

within cranial neural tube in embryos of diabetic mice, it was suggested that maternal diabetes induces neural tube malformations that are associated with altered expression of a variety of genes involved in apoptosis, proliferation, migration and differentiation of neurons.³⁵ Diabetes-induced increased neuroepithelial cell apoptosis in neural tube defects has also been associated with the over-expression of P53 gene due to diabetes-induced under-expression of Pax3 gene.^{46,47,48,49} A loss of function mutation of the Pax3 gene is responsible for the Splotch (Sp) phenotype in mice.^{50,51,52} Alterations in the expression of Hox genes have also been associated with diabetic condition.⁵³

In mice, expression of Pax3 begins in the neuroepithelium on embryonic day 8,^{5,54} a stage which coincides with the stage in human development that is sensitive to maternal diabetes-induced neural tube defects.⁴⁶ Recent studies suggest that impaired expression of Pax3 is mediated by diabetes-induced oxidative stress occasioned by the associated metabolic derangements.^{4,55,56} Mis-expression of other genes (in addition to Pax3 and P53) that regulate progenitor cell viability at critical stages of organogenesis has been advocated as a possible general mechanism for diabetes-induced embryopathies.⁵ It is possible that maternal diabetes interferes with the expression of a variety of genes and molecules that regulate important developmental processes during organogenesis, which could provide cellular and molecular explanations for the pathogenesis of diabetes-induced embryopathies.

CONCLUSION

The effects of STZ-induced IDDM on cranial neural crest cell migration and cell proliferation in malformed embryos from MF1 diabetic mice were studied. The results suggest that the normal migration of the neural crest cells may be unaltered by the diabetic state. There was also no difference in the pattern of immunoreactivity for fibronectin and laminin in the migratory pathways of the neural crest cells. However, the diabetic state may have resulted in an impairment of normal cell developmental processes as deduced from the observed distortion in the neuroepithelial cell proliferative cycle and deficit in the estimated absolute number of cells of the trigeminal ganglion in malformed embryos of the diabetic mice. It is probable that the teratogenic effects of the diabetic condition involve inhibition of both ecto-mesenchymal cell proliferation and the generation of neural crest cells from their progenitor cells. The consequent reduction in the number of neural crest cells produced and emigrating from the neural tube could explain in part the deficit in the number of crest cells homing-in on the target organs. This effect of the diabetic state on progenitor cell differentiation and cell proliferation may stem from interference with the expression of a variety of regulating genes and molecules involved in the cell developmental processes and reflect the complex nature of this disease.

ACKNOWLEDGEMENTS

This work was supported by a Commonwealth Scholarship Award, and carried out in the Department of Biomedical Science Laboratory, University of Sheffield, UK, under the supervision of Prof. Martin Atkinson.

REFERENCES

1. Martinez-Frias ML. Epidemiological Analysis of Outcomes of Pregnancy in Diabetic Mothers: Identification of the Most Characteristic and Most Frequent Congenital Anomalies. *American Journal of Medical Genetics* 1994, 51: 108-113.
2. Macintosh MCM, Fleming KM, Bailey JA, Doyle P, Modder J, Acolet D, Golightly S, Miller A; Perinatal mortality and congenital anomalies in babies of women with type 1 or type 2 diabetes in England, Wales and Northern Ireland: Population based study. *British Medical Journal* 2006, 333: 177–180.
3. Reece AE, Ciang-Dong M, Zhiyong S, Ying-King W, Danny D. Aberrant patterns of cellular communication in diabetes-induced embryopathy in rats: II, Apoptotic pathways. *American Journal of Obstetrics and Gynecology*, 2005, 192: 967–972.
4. Clapes S, Fernandez T, Suarez G, Oxidative Stress and Birth Defects in Infants of Women with Pregestational Diabetes. *MEDICC Review*. 2013, 15(1): 37–40.
5. Chappell Jr, JH, Wang XD, Loeken MR. Diabetes and apoptosis: neural crest cells and neural tube. *Apoptosis* 2009, 14: 1472–1483.
6. Versiani BR, Gilbert-Barnes E, Giuliani LR, Peres LC, Pina-Neto JM; Caudal dysplasia sequence: Severe phenotype presenting in offspring of patients with gestational and pregestational diabetes. *Clinical Dysmorphology*. 2004, 13(1): 1–5.
7. Ferencz C, Rubin JD, McCarter RJ, Clark EB. Maternal diabetes and cardiovascular malformations: Predominance of double outlet right ventricle and truncus arteriosus. *Teratology* 1990. 41: 319-326.
8. Nielsen GL, Norgard B, Puhoe E, Rothman KJ, Sorensen HT, Czeizel AE; Risk of specific congenital abnormalities in offspring of woman with diabetes. *Diabetic Medicine* 2005, 22: 693–696.
9. Chinnah, T. I. The MF1 Mouse Strain: An Animal Model of Streptozotocin-Induced Diabetes Mellitus for Studying the Mechanisms of IDDM-Induced Cardiovascular Defects. *Anatomical Society of Nigeria Journal of Anatomical Sciences* 2012, 3(1): 4–13.
10. Kirby ML, Waldo K. L. Role of neural crest in congenital heart disease. *Circulation* 1990. 82: 332-340.
11. Moerman P, Goddeeris P, Lauwerijns J, Van der Hauwaert LG. Cardiovascular malformations in DiGeorge syndrome (congenital absence or hypoplasia of the thymus). *British Heart Journal* 1980, 44: 452-459.
12. Van Mierop LDH, Kutsche LM. Cardiovascular anomalies in DiGeorge syndrome and importance of neural crest as a possible pathogenetic factor. *American Journal of Cardiology* 1986, 58: 133-137.
13. Novak RW, Robinson HB. Coincident DiGeorge anomaly and renal agenesis and its relation to maternal diabetes. *American Journal of Medical Genetics* 1994, 50: 311-312.
14. Zaw W, Stone DG; Perinatal/Neonatal Case Presentation: Caudal Regression Syndrome in Twin Pregnancy with Type II Diabetes. *Journal of Perinatology* 2002, 22: 171–174.
15. Depraetere M, Dehauwere R, Marien P, Fryns JP. Severe axial mesodermal dysplasia spectrum in an infant of a diabetic mother. *Genetic Counseling* 1995, 6(4): 303-307.
16. Martinez-Frias ML, Gomar J. New Case of Axial Mesodermal Dysplasia Sequence: Epidemiologic Evidence of a Single Entity. *American Journal of Medical Genetics* 1994, 49: 74-76.
17. Kaufman MH. Morphological stages of postimplantation embryonic development. In: Copp AJ, Cockcroft DL. (Ed): *Postimplantation Mammalian Embryos: A Practical Approach*. IRL Press, Oxford, New York, Tokyo 1990, Pages 81-90.
18. Mayhew TM. The new stereological methods for interpreting functional morphology from slices of cells and organs. *Experimental Physiology* 1991, 76: 639-665.
19. Warren MA, Bedi KS. Synapse-to-neuron ratios in the visual cortex of adult rats undernourished from about birth to 100 days of age. *Journal of Comparative Neurology* 1982, 210: 59-64.
20. Gundersen HJG. Stereology of arbitrary particles. A review of unbiased number and size estimators and the presentation of some new ones, in memory of William R. Thompson. *Journal of Microscopy* 1986, 143(1): 3-45.
21. Warren MA. Simple morphometry of the nervous system. In: *Quantitative methods in neuroanatomy* By Stewart MG (ed). Chichester, England. John Wiley and Sons Publishers 1992, Pp 211-247.
22. Gundersen HJG, Bagger P, Bendtsen TF, Evans SM, Korbo L, Marcussen N, Moller A, Nielsen K, Nyengaard JR, Pakkenberg B. The new stereological tools: Dissector, fractionator, nucleator and point sampled intercepts and their use in pathological research and diagnosis. *APMIS* 1988, 96(10): 857-881.
23. Tucker GC, Delarve M, Zada S, Boucaut JC, Thiery JP. Expression of the HNK-1/NC-1 epitope in early vertebrate neurogenesis. *Cell Tissue research* 1988, 251: 457-465.
24. Holley JA, Yu RK. Localization of Glycoconjugates Recognized by the HNK-1 Antibody in Mouse and Chick Embryos during Early Neural Development. *Dev. Neuroscience* 1987, 9: 105-119.
25. Hamburger V. Experimental Analysis of the Dual Origin of the Trigeminal Ganglion in the Chick Embryo. *Journal of Experimental Zoology* 1961, 148: 91-124.
26. D'Amico-Martel A, Noden D. Contributions of placodal and neural crest cells to avian cranial peripheral ganglia. *American Journal of Anatomy* 1983, 166: 445-468.
27. Davies AM. The trigeminal system: an advantageous experimental model for studying neuronal development. *Development*. 103(Suppl.) 1988, 175-183.
28. Simmons RA, Gounis AS, Bangalore SA, Ogata ES. Intra-uterine growth retardation: fetal glucose transport is diminished in lung but spared in brain. *Pediatric Research* 1992, 31: 59-63.
29. Bedi KS, Warren MA. The effects of undernutrition during early life on the optic nerve fibre number and size-frequency distribution. *The Journal of Comparative Neurology* 1983, 219: 125-132.
30. Hart G. Some effects of undernutrition on the

- ultrastructure of the rat sciatic nerve: A morphometric study. BSc Project. The university of Sheffield 1988.
31. Williams PL, Bannister LH, Berry MM, Collins P, Dyson M, Dussek JE, Ferguson MWJ (Eds) Gray's Anatomy. 38th Edition, Churchill Livingstone 1995, PP217-261.
 32. Boulder Committee. Embryonic vertebrate central nervous system. Revised terminology. Anatomical records 1970, 166: 257-261.
 33. Gao, Q., Gao, Y.-M., Hyperglycemic condition disturbs the proliferation and cell death of neural progenitors in mouse embryonic spinal cord. International Journal of Developmental Neuroscience 2007, 25: 349–357.
 34. Cerderberg, J., Picard, J.J., Eriksson, U.J., Maternal diabetes in the rat impairs the formation of neural crest derived cranial nerve ganglia in the offspring. Diabetologia 2003, 46: 1245–1251.
 35. Jiang, B., Kumar SD., Loh WT., Manikandan, J., Ling, E.-A., Tay, SSW., Dheen, ST., Global Gene Expression Analysis of Cranial Neural Tubes in Embryos of Diabetic Mice. Journal of Neuroscience Research 2008, 86: 3481–3493.
 36. Panchision, D. M., McKay, R. D., The control of neural stem cells by morphogenic signals. Curr. Opin. Genet. Dev. 2002, 12: 478–487.
 37. Copp, A. J., Green, N. D., Murdoch, J. N., The genetic basis of mammalian neurulation. Nat. Rev. Genet. 2003, 4: 784–793.
 38. Sommer, L., Rao, M., Neural stem cells and regulation of cell number. Prog. Neurobiol 2002, 66: 1–18.
 39. Fu J., Tay SS., Ling EA., Dheen ST., High glucose alters the expression of genes involved in proliferation and cell-fate specification of embryonic neural stem cells. Diabetologia 2006, 49: 1027–1038.
 40. Pampfer S, DeHertogh R, Vanderheden I, Michiels B, Vercheval M. Decreased inner cell mass proportion in blastocysts from diabetic rats. Diabetes 1990, 39: 471-476.
 41. Hiramatsu Y., Sekiguchi N., Hayashi M., Isshiki K, Yokota T, King GL, Loeken MR Diacylglycerol production and protein kinase C activity are increased in a mouse model of diabetic embryopathy. Diabetes 2002, 51: 2804–2810.
 42. Bogatcheva N, Verin AD, Wang P, Birukova A, Birukov K, Mirozpoyazva T, Adyshev D, Chiang E, Crow M, Garcia JG. Phorbol esters increase MLC phosphorylation and actin remodelling in bovin lung endothelium without increased contraction. Am J Physiol Lung Cell Mol Physiol 2003, 285: L415–L426.
 43. Takahashi T, Shibuya M, The overexpression of PKCdelta is involved in vascular endothelial growth factor-resistant apoptosis in cultured primary sinusoidal endothelial cells. BiochemBiophys Res Commun 2001, 280: 415–420.
 44. Randhawa PK., Rylova S., Heinz JY., Kiser S., Fried JH., Dunworth WP., Anderson AL., Barber AT., Chappell JC., Roberts DM., Bautch VL.. The Ras Activator RasGRP3 Mediates Diabetes-Induced Embryonic Defects and Affects Endothelial Cell Migration. Circulation Research 2011 108: 1199 – 1208.
 45. Schaeffer V., Hansen KM., Morris DR., Abrass CK., Reductions in laminin $\beta 2$ mRNA translation are responsible for impaired IGFBP-5-mediated mesangial cell migration in the presence of high glucose. Am J Physiol Renal Physiol 2010, 298(2): F314–F322.
 46. Phelan SA, Ito M, Loeken MR. Neural tube defects in embryos of diabetic mice: role of the pax-3 gene and apoptosis. Diabetes 1997, 46 (7): 1189-1197.
 47. Cai J, Phelan SA, Hill AL, Loeken MR. Identification of Dep-1, a new gene regulated by the transcription factor Pax-3, as a marker for altered embryonic gene expression during diabetic pregnancy. Diabetes 1998, 47: 1803-1805
 48. Fine EL, Horal M, Chang TI, Fortin G, Loeken MR. Evidence that elevated glucose causes altered gene expression, apoptosis and neural tube defects in a mouse model of diabetic pregnancy. Diabetes 1999, 48: 2454-2462.
 49. Loeken MR., Advances in understanding the Molecular Causes of Diabetes-Induced Birth Defects. Journal of Society for Gynecologic Investigation 2006, 13: 2 – 10.
 50. Epstein DJ, Vogan KJ, Trasler DG, Gros P. A mutation within intron 3 of the Pax-3 gene produces aberrantly spliced mRNA transcripts in the splotch (Sp) mouse mutant. Proceedings of National Academy of Science, USA 1993, 90: 532-536.
 51. Goulding MD, Lumsden A, Cruss P. Signals from the notochord and floor plate regulate the region-specific expressions of two Pax genes in the developing spinal cord. Development 1993, 117(3): 1001-1016.
 52. Chalepakis G, Jones FS, Edelman GM, Gruss P. Pax-3 contains domains for transcription activation and transcription inhibition. Proceedings of National Academy of Science, USA 1994, 91: 12745-12749.
 53. Jacobs H, Bogue CW, Pinter E, Wilson CM. Fetal lung mRNA of Hox genes are differentially altered by maternal diabetes and butyrate in rats. Pediatric Research 1998, 44(1): 99-104.
 54. Goulding MD, Chalepakis G, Deutsch U, Erselius JR, Gruss P. Pax-3, a novel murin DNA binding protein expressed during early neurogenesis. EMBO Journal 1991, 10: 1135-1147.
 55. Morgan SC., Relaix F., SandellLL., Loeken MR., Oxidative Stress during Diabetic Pregnancy Disrupts Cardiac Neural Crest Migration and Causes Outflow Tract Defects. Birth Defects Research (Part A) 2008, 82: 453–463.
 56. Roest PAM, van Iperen L., Vis S., Wisse LJ., Poelmann RE., Steegers-Theunissen RPM, Molin DGM., Eriksson UJ., Gittenberger-De Groot AC., Exposure of Neural Crest cells to Elevated Glucose Leads to Congenital Heart Defects, an Effect that can be prevented by N-Acetylcysteine. Birth Defects Research (Part A) 2007, 79: 231–235.